

A New Diagram for the Application of Welding Theories

Developed to promote comprehension of welding theories, the new diagram relates welding variables to thermal history, mechanical properties and macrostructure of the weld

BY G. H. HARTH AND W. C. LESLIE

ABSTRACT. This article attempts to integrate welding theories and empirical welding relationships with the aid of a diagram. The diagram is a graph of Log H vs Log S. H is the familiar energy absorbed per unit length of weld, and S is the welding traverse speed. Various welding relationships can be readily plotted and comprehended on the new diagram. It enables one to visualize simultaneously the interrelationship between the various important welding variables and the effects of these variables on the thermal history, macrostructure, and the properties of the weld.

Introduction

A review of the welding literature published over the past thirty years reveals some confusion concerning the influence of various welding variables on the thermal history, the macrostructure, and the properties of a weld. One of the main difficulties in fully understanding the interrelation of the variables and their relationship to the weld arises from the large number of variables and their complex interrelationships.

The major welding variables that have been identified and studied include welding current, arc-gap

voltage, applied (available) power, absorbed power, heat transfer efficiency (ratio of absorbed power to applied power), power density, travel speed, and energy per unit length of weld. Researchers have determined the effects of each of these variables on such things as maximum hardness and strength of the weld metal, cooling rate, molten metal (nugget) cross-sectional area, and dwell time at elevated temperatures during welding.

However, while these relationships have been developed and are available, it is not easy to recognize interaction between these variables. As an example, Jackson and Goodwin (Ref. 1) have demonstrated that the nugget area of a weld increases as travel speed increases if the energy per unit length of weld is held constant. (See Fig. 1). The practical welding engineer would like to know how this increased travel speed would also affect the maximum cooling rate in the weld and the hardness and strength of the weld. He would also like to know how a particular welding process modifies these relationships. It would be advantageous to have a diagram from which this information could be obtained easily and simultaneously.

This paper presents a basic diagram which is intended to promote understanding of the welding situation. The unique feature of this diagram is that it enables one to comprehend the interrelationships of the major welding variables and their combined effects on the weld zone. While the diagram can not predict specific welding phenomena with

marked accuracy, it can indicate trends in relationships and it can be used to estimate the effects of welding variables on welding phenomena. The diagram can be easily modified to suit the needs of the particular welding situation.

Background

Development of Welding Theories

Rosenthal (Ref. 2) originally developed the theoretical heat transfer equations which relate welding parameters to the thermal history of a bead-on-plate weld. He used the point source theory of Carslaw and Jaeger (Ref. 3) for heat conduction in solids. Christensen and Davies (Ref. 4) further manipulated the theoretical equations of Rosenthal to yield nondimensional diagrams of interest to a welding engineer. These diagrams were developed for predicting trends in the relationship between welding variables and such important metallurgical aspects as the temperature histories at various locations within a weld, the cross-sectional area of molten metal in a weld, and the depth of weld penetration. Figure 2 shows one of the nondimensional diagrams of Christensen and Davies.

The diagram was simplified by Christensen and Davies through the use of nondimensional coordinates. An operating parameter, n , is used and defined as

$$n = \frac{QS}{12.6 a^2 cp(T_c - T_0)} \quad (1)$$

where Q is the absorbed power and S

G. H. HARTH, formerly Research Assistant at The University of Michigan, is now Senior Welding Engineer with Babcock and Wilcox, Barberton, Ohio.

W. C. LESLIE is Professor of Materials and Metallurgical Engineering at The University of Michigan.

List of Symbols

A	welding current
a	average thermal diffusivity
B_1	constant = $-6.28 K(T_1 - T_0)^2$
C_1	cooling rate at T_1
c	average specific heat
H	energy absorbed per unit length of weld
K	thermal conductivity
N	nugget area (see Eq. 3)
NA	nondimensional area (see Eq. 2)
n	operating parameter (see Eq. 1)
p	average density of metal
Q	absorbed power (absorbed by plate and weld)
Q_s	power of the source (available power)
R	maximum HAZ hardness
S	welding speed
T_c	critical temperature (temperature of interest)
T_0	plate temperature prior to welding
T_1	temperature of interest
V	welding arc voltage drop
YS	yield strength of the weld
Z	arc heat transfer efficiency factor

is the welding traverse speed. In Fig. 2 the nondimensional nugget area, NA, is defined as

$$NA = \frac{NS^2}{4a^2} \quad (2)$$

where N is the actual nugget area.

The graphical display of theoretical relationships developed by Christensen and Davies allows graphical solutions to theoretical welding equations and bypasses much of the burdensome calculations normally associated with welding theory. These diagrams were therefore major steps towards making welding theory more easily understood and useful. However, they are still complex enough to inhibit their direct use in practical welding situations without some further development.

The limitations of the point source theory used by Rosenthal and by Christensen and Davies are discussed in detail by Meyers et al (Ref. 5). The authors compared the welding theories to actual welding data, and concluded that the theory is excellent for predicting trends in welding situations. It is also excellent for predicting the thermal history and metallurgical response at slow to moderate welding speeds and at points some distance from the welding heat source (arc). The theory, however, is inaccurate at fast welding

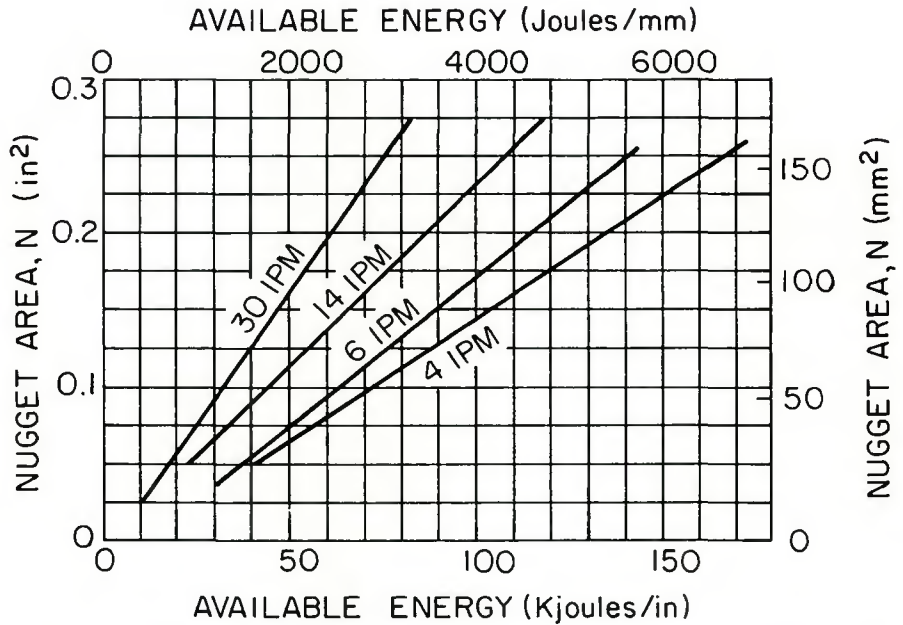


Fig. 1 — Relation of the weld nugget area to traverse speed and available energy (after Jackson and Shrubbsall, Ref. 6)

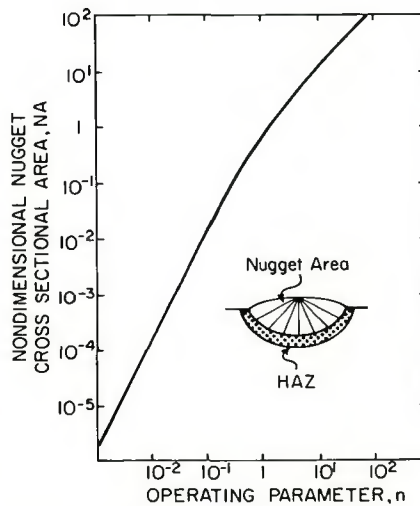


Fig. 2 — Theoretical curve relating the weld nugget nondimensional cross-sectional area to the operating parameter (after Christensen and Davies, Ref. 4)

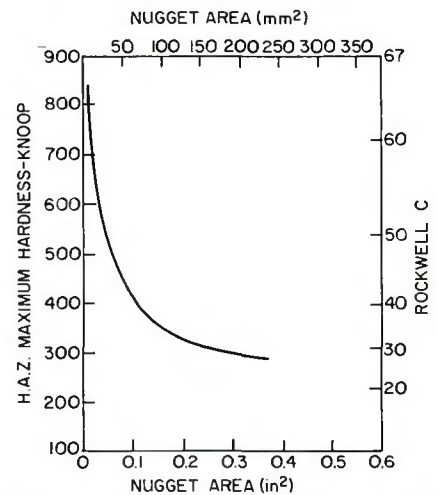


Fig. 3 — Relation of nugget area to maximum hardness in the HAZ for AISI 1045 carbon steel (after Schultz and Jackson, Ref. 7)

speeds and at points close to the heat source.

This conclusion is not surprising, because the theory assumes a point source of heat instead of the three-dimensional welding arc (heat source) normally encountered in welding. The theory is also limited by assuming a hemispherical HAZ (or hemispherical isotherms) in thick plates.

Development of Empirical Welding Relationships

While Rosenthal and Christensen and Davies were developing the theoretical equations for bead-on-plate welding, Jackson and co-workers (Refs. 1,6,7) and Dorschu

(Ref. 8) were experimentally determining the relationship of welding variables to weld zone thermal history, macrostructure, and properties. Some of their findings are shown in Figs. 1 and 3-5.

Shultz and Jackson (Ref. 7) also developed an empirical equation which is quite useful for predicting the nugget area of a weld. The equation is

$$N = 3.33 \times 10^{-2} \frac{A^{1.55}}{S^{0.903}} \quad (3)$$

where A is the welding current in amperes, S is in mm/sec, and N is in mm².

*See Index of Symbols

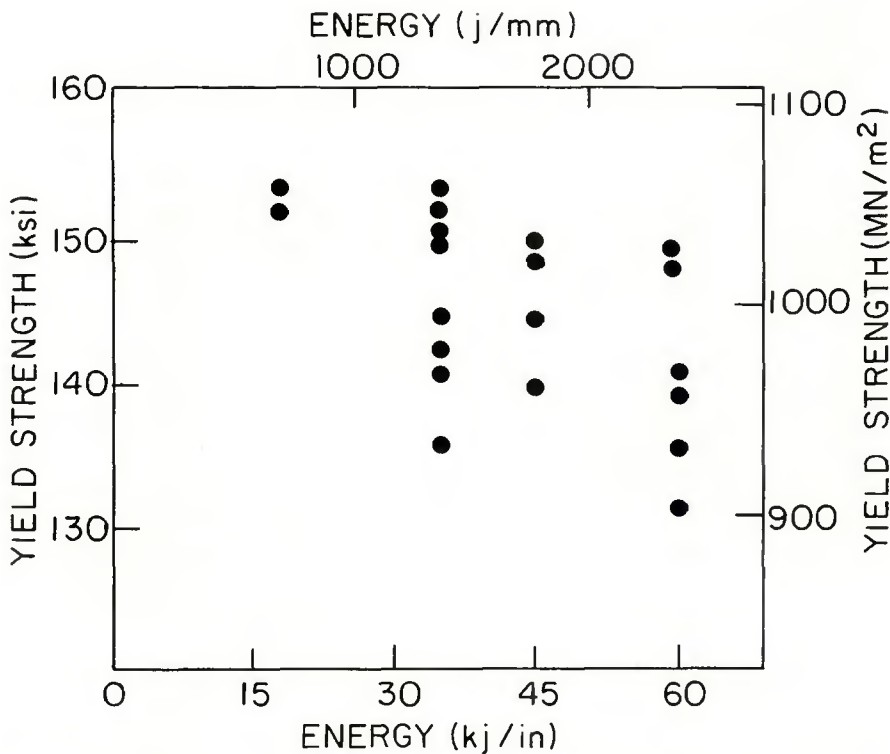


Fig. 4 — Relation between yield strength and available energy (after Schultz and Jackson, Ref. 7)

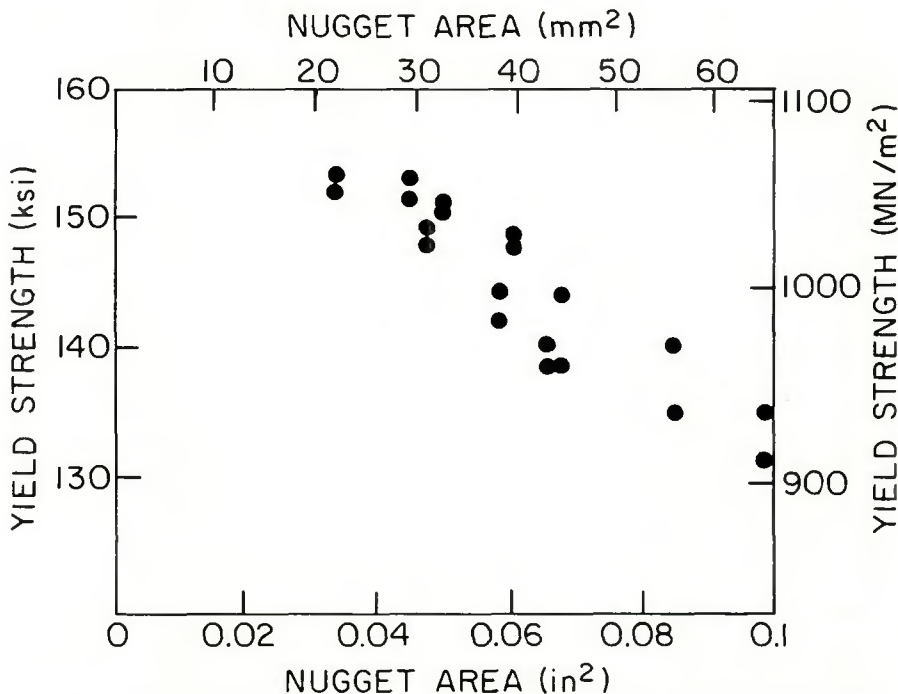


Fig. 5 — Relation between measured weld nugget area and yield strength for E14018 high-strength multipass weld metal (after Schultz and Jackson, Ref. 7)

By combining Equation 3 with data of the type displayed in Figs. 3 and 5, one can relate some welding variables to the maximum HAZ hardness and the weld strength. Equation 3 is limited, however, in that it does not compensate for the effects of weld preheat, and it is subject to some errors if applied to various welding

processes (Ref. 6). Equation 3 also does not aid in predicting the maximum cooling rate in a weld.

All of the relationships that have been developed and discussed in the present article are, in themselves, useful tools for the welding engineer. One of the obvious problems with all of them is that they are interrelated in

Table 1 — Arc Heat Transfer Efficiency as a Function of Welding Process (after Christensen and Davies, Ref. 4)

Welding process	Heat transfer efficiency, Z, on Steel, %
Submerged arc welding	0.90-0.99
Shielded metal-arc welding	0.66-0.90
Gas metal-arc welding	0.66-0.69
Gas tungsten-arc welding	0.22-0.48

a complex fashion, as mentioned in our previous example; and one graph or a group of graphs can not show the total interaction of all of the welding variables. One of the hindrances to progress in useful application of welding theory and welding data developed to date is that it is usually not easily applied. A better method of presenting theoretical and experimental information is desirable.

Development and Use of the Diagram

Power Definition

A point to remember in using the theories of Rosenthal and of Christensen and Davies is that the power term, Q , which appears in the theoretical equations (and on the nondimensional plots of Christensen and Davies) is the absorbed power, not the power of the source, Q_s . In order to translate the power of the source, Q_s , into the power absorbed by the welded plate, Q , the heat transfer efficiency factor, Z , is required.

Thus,

$$Q = ZQ_s = ZAV \quad (4)$$

There has been some controversy over the value of Z , and it is not certain that Z is a constant for a given welding method, arc length, or traverse speed. However, Christensen and Davies (Ref. 4) have discussed and calculated the relative value of Z for particular welding processes, and this data is presented in Table 1. Z is important in the use of our new diagram in that it is used to judge how a change in welding process affects the welding situation. Any change in welding process will obviously change the value of Z .

Development of Log H vs Log S Diagram

The energy deposited per unit length of weld, H , is given by

$$H = ZQ_s/S \quad (5)$$

Equation 5 is one of the most fundamental welding equations, relating four of the major welding variables.

Taking the log of both sides:

$$\log H = \log (ZQ_s) - \log S \quad (6)$$

Equation 6 is the basis for the new diagram shown in Fig. 6. It is produced by plotting lines of constant ZQ_s (absorbed power) on the log H vs log S graph.

The diagram in Fig. 6 shows the interrelationship of the energy per unit length, H, the traverse speed, S, the heat transfer efficiency, Z, and the power of the source, Q_s . If the electrode diameter and Z remain constant for a given welding process, then the direction indicated in Fig. 6 as increasing ZQ_s can also be thought of as the direction of increasing power density.

Figure 7 shows theoretical predictions of the weld nugget area as it relates to the weld variables. Lines of constant nugget area (N_1 and N_2) have been plotted as examples. Alternatively, we could have used the empirical relationship developed by Jackson and Shrubbsall to accomplish the same results as developed theoretically and shown in Fig. 7.

The importance of Fig. 7 is that such diagrams can be used to predict the weld macrostructure which will result from given combinations of arc power, traverse speed, and welding process (Z). To demonstrate its use, we can predict the change in nugget area produced by a change in traverse speed at constant H. At constant H, an increase in S (requiring an appropriate increase in Q_s) will increase the size of the weld nugget from N_2 to N_1 .

Note that we have increased the nugget area and have not changed the maximum cooling rate of the weld, since constant H results in constant C_1 . Some researchers have suggested that the nugget area controls the cooling rate (Ref. 7 and 10). Heat transfer equations adequately predict trends in the cooling rates without assuming a weld nugget (Ref. 4 and 5).

Weld Properties and the Diagram

Figures 3 and 5 present data which indicate that the yield strength and maximum HAZ hardness of a weld can be correlated to the weld nugget cross-sectional area. It can be noted that the yield strength and maximum HAZ hardness of a given weld increase as the nugget area decreases. These empirical relationships can be used to plot lines of constant hardness, R, and constant yield strength, YS, in the same way that we have plotted theoretical lines of constant area on Fig. 7. We have shown an example of this in Fig. 7.

Hardness and yield strength of a given steel are not simple functions of cooling rate or energy per unit length; they are complex functions of cooling rate and traverse speed, as shown in Fig. 7. It is now obvious that the yield strength of the weld can not be cor-

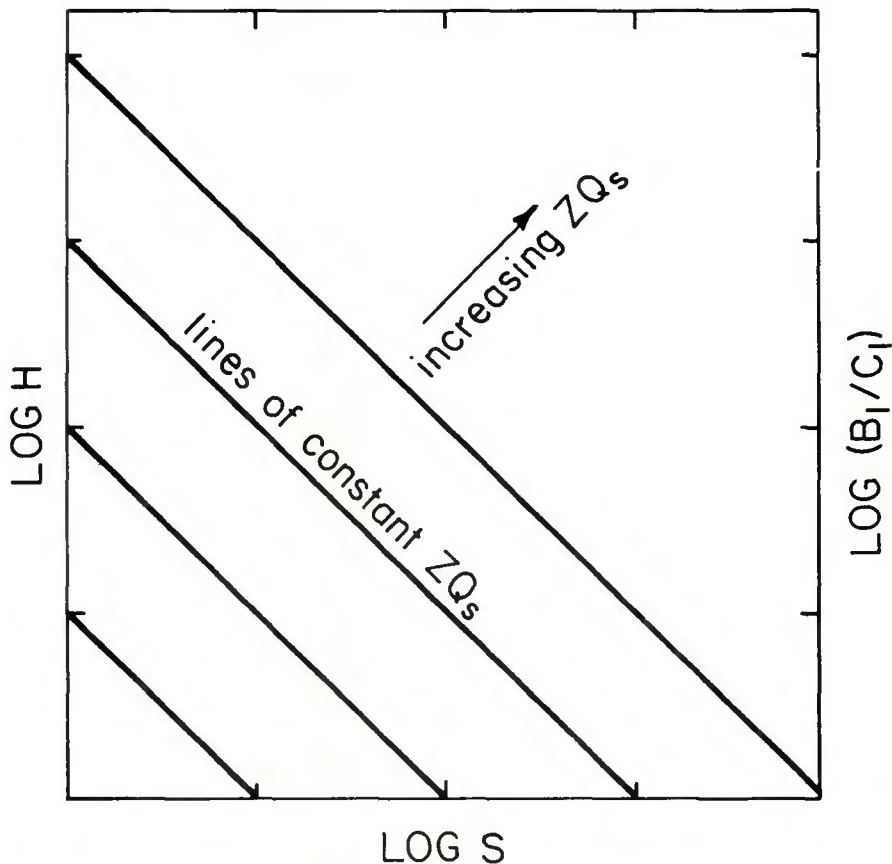


Fig. 6 — Basic diagram developed by plotting lines of constant ZQ_s on a graph of log H vs log S

related to the energy deposited per unit length, as attempted in Fig. 4. Hardness and strength are determined by composition, grain size, and thermal history. Weld nugget area is a good indication of conditions which combine to produce a given hardness and strength.

Time at elevated temperatures increases with slower traverse speeds at a given value of H and C_1 . Longer times at elevated temperatures cause increased grain growth, increased dissolution of carbides, and increased homogeneity of composition. These factors increase the hardenability and strength of steels. Consequently, the properties of the weld are not solely functions of the cooling rate or of the energy deposited per unit length.

As we move to the left in Fig. 7 and follow a line of constant area (e.g., N_1), we note that the time at a given temperature in the weld increases and the cooling rate decreases. These two influences combine and are partially self compensating such as to moderate or nullify changes in hardness and strength within the weld zone as we follow a constant nugget area line. Thus, nugget area is an indirect indicator of hardness and strength although it does not determine either of these directly.

Nonferrous alloys and austenitic stainless steel probably would not follow the trends indicated in Figs. 3, 4, 5, and 7, and their constant hardness and constant yield strength curves might be far different from those shown in Fig. 7.

Figure 7 represents only one of several possible ways that the log H vs log S diagram can be used to comprehend the complex interaction of welding variables with the thermal history, weld macrostructure, and the properties of the weld. The welding equations developed by Christensen and Davies can be used to predict the depth of weld penetration, width of the HAZ, dwell time at elevated temperatures etc. This information can be plotted on the log H vs log S diagram and combined with empirical data to aid in the understanding and prediction of welding phenomena.

Z and the Diagram

Some researchers (Ref. 7) suggest that the nugget area is a measure of heat transfer efficiency, Z. The heat required to melt a volume of metal equivalent to a unit length of the weld nugget is divided by the heat per unit length available from the arc to obtain their measure of efficiency. By this definition, increases in nugget area (nugget volume/unit length) at

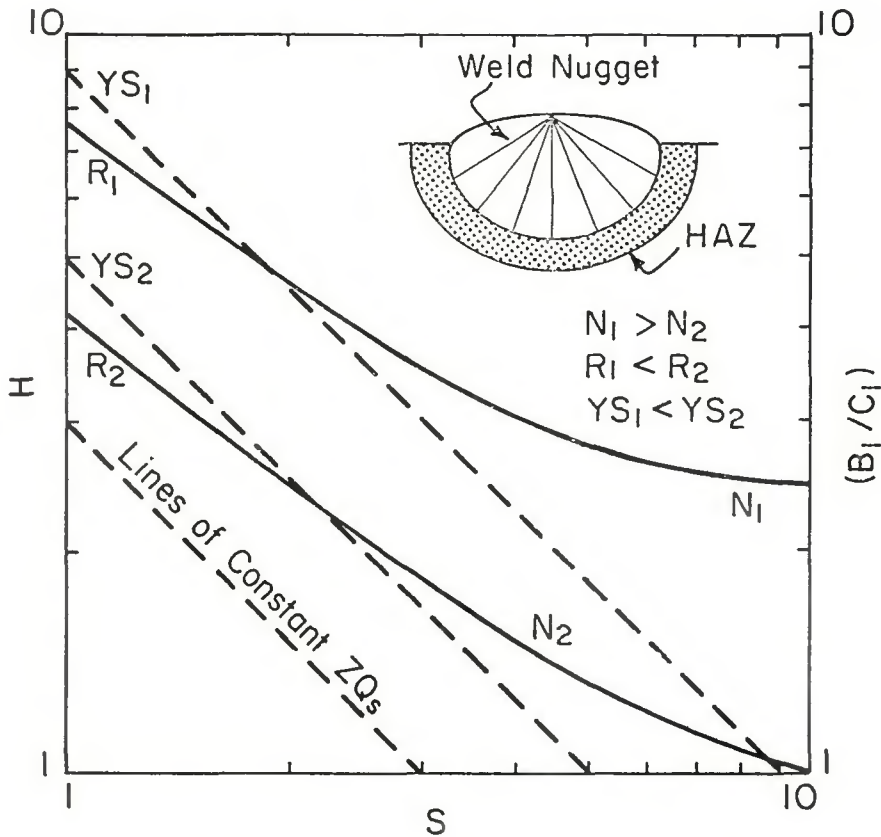


Fig. 7 — Log H vs log S diagram modified to include theoretical curves of nugget cross-sectional area, N, maximum HAZ hardness, R, and yield strength of the weld, YS

constant available heat per unit length indicate increases in heat transfer efficiency.

From Fig. 7 It is obvious that the nugget area, N, can be increased at constant H and Z by simultaneously increasing S and Q_s . An increase in the nugget area associated with an increase in S at constant H does not signify an increase in arc heat transfer efficiency, Z. Therefore, nugget area is not a measure of the heat transfer efficiency, Z.

The increase of nugget area with increasing traverse speed at constant H can be understood as follows:

Heat is rapidly dissipated in the mass of the plate at slow traverse speeds without melting much metal. At higher traverse speeds and constant H (increased Q_s), the rate of heat input to the plate and weld is higher; and therefore, the molten zone naturally increases in size. Ac-

cording to the point source theory, heat transfer efficiency across the arc, Z, has nothing to do with the increase in nugget area associated with increased traverse speeds at constant H.

Barry et al, (Ref. 9) also used the nugget area as a measure of efficiency; however, they correctly defined their efficiency as a percentage of total absorbed heat used to create a molten nugget. This efficiency then is not related to Z in the welding theories.

We have developed a diagram of log H vs log S by combining a basic welding relationship with welding heat transfer theories and some experimental data. It can be used to indicate how the various welding variables interact and affect the thermal history, macrostructure, and properties of a bead-on-plate weld.

The log H vs log S diagram is as ac-

curate in predicting the thermal history, macrostructure, and properties of a weld as the current welding theories and welding data will permit. These welding theories are suited for predicting trends and for approximating specific data. As new information is developed which can modify and increase the accuracy of the current welding theories and data, the accuracy and potential of the log H vs log S diagram will increase.

Acknowledgments

The information presented in this article was obtained during a study conducted under a grant from the General Motors Corporation, Manufacturing Development, General Motors Technical Center. The authors wish to express their gratitude to Metals Engineering of Manufacturing Development for this aid to their research.

References

1. Jackson, C. E., and Goodwin, W. J., "Effects of Variations in Welding Technique on the Transition Behavior of Welded Specimens — Part II," *Welding Journal*, 27(5), May 1948, Res. Suppl., 253-s to 266-s.
2. Rosenthal, D., "Mathematical Theory of Heat Distribution During Welding and Cutting," *Welding Journal*, 20(5), May 1941, Res. Suppl., 220-s to 225-s.
3. Carslaw, H. S., and Jaeger, J. C., *Conduction of heat in Solids*, Clarendon Press, Oxford (1959).
4. Christensen, N., and Davies, V., "Distribution of Temperatures in Arc Welding," *British Welding Journal*, 12(2), 54 to 75 (1965).
5. Myers, P. S. et al, "Fundamentals of Heat Flow in Welding," *Welding Research Bulletin*, No. 123, Welding Research Council, N.Y. (1967).
6. Jackson, C. E., and Shurbsall, A. E., "Energy Distribution in Electric Welding," *Welding Journal*, 29(5), May 1950, Res. Suppl., 231-s to 241-s.
7. Shultz, B. L., and Jackson, C. E., "Influence of Weld Bead Area on Weld Metal Mechanical Properties," *Welding Journal*, 52(1), Jan. 1973, Res. Suppl., 26-s to 37-s.
8. Dorsch, K. E., "Control of Cooling Rates in Steel Weld Metal," *Welding Journal*, 47(2), Feb. 1968, Res. Suppl., 49-s to 62-s.
9. Barry, J. M. et al, "Heat Conduction from Moving Arcs in Welding," *Welding Journal*, 42(3), March 1963, Res. Suppl., 97-s to 104-s.
10. Stout, R. D., and Doty, W. D., *Weldability of Steels*, Welding Research Council, N.Y., N.Y. (1971).

Authors — a reminder

Abstracts with application forms (page 213, March issue) for papers to be presented at the 1976 Brazing and Soldering Conference in St. Louis must be mailed by September 15, 1975

WRC Bulletin

No. 187

Sept. 1973

"High-Temperature Brazing"

by H. E. Pattee

This paper, prepared for the Interpretive Reports Committee of the Welding Research Council, is a comprehensive state-of-the-art review. Details are presented on protective atmospheres, heating methods and equipment, and brazing procedures and filler metals for the high-temperature brazing of stainless steels, nickel base alloys, superalloys, and reactive and refractory metals. Also included are an extensive list of references and a bibliography.

The price of WRC Bulletin 187 is \$5.00 per copy. Orders should be sent to the Welding Research Council, 345 East 47th Street, New York, N.Y. 10017.

WRC Bulletin

No. 197

August 1974

"A Review of Underclad Cracking in Pressure-Vessel Components"

by A. G. Vinckier and A. W. Pense

This report is a summary of data obtained by the PVRC Task Group on Underclad Cracking from the open technical literature and privately sponsored research programs on the topic of underclad cracking, that is, cracking underneath weld cladding in pressure-vessel components. The purpose of the review was to determine what factors contribute to this condition, and to outline means by which it could be either alleviated or eliminated. In the course of the review, a substantial data bank was created on the manufacture, heat treatment, and cladding of heavy-section pressure-vessel steels for nuclear service.

Publication of this report was sponsored by the Pressure-Vessel Research Committee of the Welding Research Council. The price of WRC Bulletin 197 is \$5.50. Orders should be sent to the Welding Research Council, 345 E. 47th St., New York, N.Y. 10017.